CARBON MONOXIDE LASER

Robert E. Center

Avco Everett Research Laboratory

Prepared for:

Advanced Research Projects Agency
Office of Naval Research

July 1972

CARBON MONOXIDE LASER

SEMI-ANNUAL TECHNICAL REPORT

prepared by

AVCO EVERETT RESEARCH LABORATORY
a division of
AVCO CORPORATION
Everett, Massachusetts

July 1972

Contract No. N00014-72-C-0030

supported by

ADVANCED RESEARCH PROJECTS AGENCY
DEPARTMENT OF DEFENSE

monitored by

OFFICE OF NAVAL RESEARCH

FOREWORD

ARPA Order No.:	1807
Name of Contractor:	Avco Everett Research Laboratory
Effective Date of Contract:	1 November 1971
Contract Expiration Date:	30 December 1972
Amount of Contract:	$201,220
Contract Number:	N00014-72-C-0030
Principal Investigation and Phone Number:	Dr. Robert E. Center Area Code 617, 389-3000, Extension 593
Scientific Officer	Director, Physics Program, Physical Sciences Division Office of Naval Research Department of the Navy Arlington, Virginia 22217
Short Title of Work:	Carbon Monoxide Laser

SUMMARY

The main objective of this program is the investigation of pulsed electrical CO lasers to determine their potential scaling to large scale, high power operation. The program is based on the application of the electron beam ionizer-sustainer concept to the vibrational excitation of CO with temperature controlled operation.

The following areas of investigation are included in the current contract:

1) Investigation of the electron beam current requirements and the E/p range for sustainer discharge excitation of CO and CO/N_2 mixtures.
2) Design and construction of the electron gun and laser cavity for operation at gas temperatures from $100^{\circ}K$ to $300^{\circ}K$.
3) Experimental investigation of the multiline/multimode operation over a range of gas temperature and pressure up to the equivalent of one atmosphere at room temperature.
4) The extension of the theoretical model to the directly excited CO laser including calculations of the transient gain and power.

During the first six months of the contract the following technical results were achieved:

1) Measurement of the electron-ion recombination rates in CO plasmas at pressures of up to one atmosphere and average electron energies from 0.2 to 0.7 eV.

2) The design and construction of a 1 meter long by 20 cm wide electron beam and power supply. Initial performance tests have yielded current densities up to 100 mamp/cm^2.

3) The design and construction of a 20 liter cavity with temperature controlled discharge electrodes and a variable temperature gas supply which can be cooled to approximately 100^{o}K.

4) Construction and testing of a 45 kjoule capacitor bank and crowbar assembly for use with the sustaining discharge.

5) Extension of existing theoretical models for steady state CO lasers to the case of a uniformly excited pulsed CO laser.

Considerable delays were experienced in the fabrication of the variable temperature discharge electrodes, in particular the multi-tube porous cathode assembly. These delays resulted from vendor problems in the laser drilling of .010 inch holes in the thin wall cathode tubes and resulted in a one month setback in the program.

I. INTRODUCTION

The CO laser program has the objective of investigating the performance characteristics of the pulsed electrical CO laser using the electron beam-sustainer discharge excitation scheme. The experimental investigation is intended to cover a wide variation in gas temperature, from 100°K to 300°K to observe the expected enhancement of the lasing output with decreasing translational temperature. The development of a theoretical model of the complex multi-vibrational level system is included in the overall program to provide support for the design of the apparatus and the interpretation of the experiments.

The following areas of investigation are included in the current contract:

1) Investigation of the electron beam current requirements and the E/p range for sustainer discharge excitation of CO and CO/N_2 mixtures.

2) Design and construction of the electron gun and laser cavity for operation at gas temperatures from 100°K to 300°K.

3) Experimental investigation of the multiline/multimode operation over a range of gas temperature and pressure up to the equivalent of one atmosphere at room temperature.

4) The extension of the theoretical model to the directly excited CO laser including calculations of the transient gain and power.

During the first six months of the contract the following technical results were achieved:

1) Measurement of the electron-ion recombination rates in CO plasmas at pressures of up to one atmosphere and average electron energies from 0.2 to 0.7 eV.

2) The design and construction of a 1 meter long by 20 cm wide electron beam and power supply. Initial performance tests have yielded current densities up to 100 mamp/cm^2.

3) The design and construction of a 20 liter cavity with temperature controlled discharge electrodes and a variable temperature gas supply which can be cooled to approximately 100^{o}K.

4) Construction and testing of a 45 kjoule capacitor bank and crowbar assembly for use with the sustaining discharge.

5) Extension of existing theoretical models for steady state CO lasers to the case of a uniformly excited pulsed CO laser.

Considerable delays were experienced in the fabrication of the variable temperature discharge electrodes, in particular the multi-tube porous cathode assembly. These delays resulted from vendor problems in the laser drilling of .010 inch holes in the thin wall cathode tubes and resulted in a one month setback in the program.

II. 500 JOULE/PULSE EXPERIMENT

An experimental CO laser has been designed and built with the ultimate aim of producing 500 joules/pulse multimode output energy in approximately 50 to 500μ secs. A schematic of the device is shown in Fig. 1 and a photograph in Fig. 2. The entire laser assembly includes the following components:

1). One meter long by 20 cm wide electron beam source designed for operation up to 100 mamps/cm^2 at electron energies up to 150 kV being supplied by a 1.5μF capacitor bank with a 0-200 kV charging power supply.

2) Control circuitry for pulse modulating the electron beam current.

3) A 45 kjoule capacitor bank with an ignitron crowbar capable of operation in the voltage ranges 0-20 kV, 0-40 kV, 0-60 kV.

4) Temperature controlled anode and cathode electrodes for the sustaining discharge. The cathode was designed as a semi-porous structure so that it can be used as the gas source, the gas being passed through a heat exchanger before entry to the cathode.

5) An evacuable cavity box to house the discharge electrodes and cavity optics. This structure is connected to a 120 cfm pump for the continuous flow of gas during the laser operation.

6) Multimode optical cavity employing a hole coupled mirror for the extraction of energy. Both 10% and 33% coupling mirrors are available.

The entire apparatus (Items (1) through (6)) was built and assembled by the end of the first 1/2 year. Initial performance tests were made on the electron gun assembly and current densities of up to 100 mamps/cm^2 were obtained at 130kV. The entire construction program was delayed by over a month due to vendor supply problems with the discharge electrodes. The main problems were with the laser drilling of the thin walled tubing for use as the porous cathode.

III. DISSOCIATIVE RECOMBINATION MEASUREMENTS

In the large volume electron beam sustained discharge, the main process limiting the electron density is the recombination of electrons with the molecular position ions. Previous experiments in both noble gases and several diatomic molecules have shown that the electron-ion recombination process is probably dominated by dissociative recombination[1] in which the electron is trapped with the subsequent formation of two neutral atoms or molecules. These measurements have been made at low pressures, up to several Torr, and have indicated room temperature recombination rate coefficients in the range 10^{-7} to 10^{-6} $cm^3/sec.$[1] Experiments in nitrogen,[2] oxygen[3] and nitric oxide[4] have demonstrated that dimer ions, such as N_4^+, exhibit larger recombination coefficients than the monomer ions at room temperature. These dimer ions are formed in termolecular reactions at higher pressures. It is evident therefore that low pressure measurements cannot by themselves be used to indicate the effective recombination rate coefficient under high pressure discharge conditions.

The present report describes measurements of the effective electron-ion recombination rates in high pressure CO discharges with CO pressures up to 1 atmosphere and electron temperatures varying from .2 to .7 eV, the ion and neutral temperature being approximately $300^{\circ}K$. These measurements are of interest in the high pressure electric CO laser. Previous measurements of electron-ion recombination

in CO have been limited to low pressure. Mentzoni and Donohoe[5] using microwave diagnostics in a plasma afterglow measured an electron-ion recombination rate of 6.8×10^{-7} cm^3/sec at room temperature. They also measured the recombination rate at 77.5°K and deduced that the recombination rate was independent of pressure up to 2 Torr [6] at this temperature.

Recently, Chong and Franklin[7] and McDaniel et. al.[8] have measured the three body rate for the conversion of CO^+ into the dimer ion $C_2O_2^+$ at room temperature. This rate is large, of the order of 10^{-28} cm^6/sec, and based on the measured equilibrium constant of 1482, referred to the standard atmosphere, it is clear that the dimer ion will dominate the monomer ion at pressures above 1 Torr at room temperature. The absence of a detectable variation of the recombination rate with pressure in the high temperature experiment of Mentzoni and Donohoe[6] may be interpreted as resulting from the breakup of the weakly bound dimer ion at high temperature. However, the dimer ion is expected to be important in the high pressure electric CO lasers which are usually operated at or below room temperature.[9,10] It should be pointed out that the expected average ion energy in excess of the thermal values in these lasers is insignificant, based on the mobility measurements of McDaniel et. al.,[8] over the anticipated range of E/N of less than 5×10^{-16} volt-cm^2 for the high pressure electric CO laser.

Although it would be desirable to mass identify the positive ions taking part in the recombination process, this was not done in the present experiments because of the extreme difficulty of mass sampling

from such high pressure systems without destroying or altering the ion composition in the sampling process. Although ion sampling has been achieved at pressures up to 70 Torr, this has involved the development of very large nozzle flow sampling systems,[11] and this was beyond the scope of the present work.

EXPERIMENTAL METHOD AND PROCEDURE

An electron beam-sustained discharge is used to create the plasma in the gas. This technique has been used recently in the development of high pressure large volume CO and CO_2 gas lasers. A schematic of the apparatus is shown in Fig. 3. A hundred kilovolt electron beam is used to ionize the gas and so create a plasma of secondary electrons with a typical density of the order of 10^{12} per cm^3. The energy of the secondary electrons is controlled by a sustaining discharge as shown in Fig. 3 in which a uniform electric field is applied across the gas. A broad area electron beam (10cm x 10cm) is employed to produce uniform ionization in the gas thereby minimizing transverse gradients and diffusion effects. The principle of the experiment is to pulse the electron beam on and off with a square profile and to monitor the temporal variation in the electron current and hence the electron density in the ionization portion and the afterglow produced by the pulsating electron beam. Since the electron density is determined by a balance between the production and loss mechanism, it is therefore possible to extract the electron ion recombination rate from the temporal variation in the electron density.

The sustaining discharge is produced between two broad area electrodes one of which, the cathode, is porous and is mounted over an aluminum foil to allow the electron beam to penetrate into the discharge region. The electron energy is chosen to be high enough to provide uniform energy deposition in the region between the discharge

electrodes which was 5 cm in the present experiment. This distance is small compared to the range of the primary electrons which is approximately 15 cm at a density of one amagat[12] and varies inversely with density. Electrostatic probes are used to monitor the electric field in the discharge region. This is necessary because the cathode fall and anode fall cannot be predicted a priori and may be expected to vary with the gas density. The discharge current density was monitored by measuring the current to an isolated button in the center of the anode. The applied electric fields were in the range from 500 volts/cm to 5000 volts/cm and for the gas pressures from 100 Torr to 700 Torr, the E/N range of the experiment was from 2×10^{-17} volt-cm^2 to 2×10^{-16} volt-cm^2. This corresponds to an average electron energy from 0.2 to 0.7 eV. Under these conditions the electron energy is coupled mainly to the vibrational degree of freedom and the translational/rotational temperature is not expected to increase by more than 20°K in the timescale of the experiment, approximately 100μ sec.

The entire discharge volume was evacuated by means of a cold trapped diffusion pump and subsequently charged to the required pressure with CO via a cold trap. The purity of the gas proved to be a significant problem in these experiments. Some early measurements indicated the attachment of electrons to some impurity in the CO supply. Because of the relatively low electron energy in these experiments dissociative attachment to CO is expected to be insignificant. Varying grades of carbon monoxide were used and no correlation was observed between the rate of attachment and the stated purity of the gas supply. Iron pentacarbonyl, $Fe(CO)_5$, was suspected as the attaching impurity since measurements by Lee[13] had indicated a very large attachment cross

section for low energy electrons to the carbonyl. The presence of the carbonyl in some of the CO cylinders was verified by I. R. absorption spectroscopy and one cylinder of Matheson UHP CO showed 50 ppm of the carbonyl. This impurity content resulted in good agreement between experimental and theoretical discharge currents assuming the attachment rates observed by Lee.[13] Subsequent removal of the $Fe(CO)_5$ either by the use of an in-line cold trap or by heating the gas to 600°C (thereby breaking the CO bonds in the carbonyl) resulted in a dramatic increase in the discharge current. Liquid nitrogen cold traps proved to be not as effective in freezing out the carbonyl as a cold trap at -90°C. The reasons for this are not known although no further attempt was made to improve or vary the design of the cold trap. It should be pointed out that the cold trap did not remove all the carbonyl as evidenced by some attachment characteristics of the electron density measurements indicating the presence of the order of one ppm of the carbonyl in the gas. Both Matheson and Linde CP grade CO were used in the final experiments since they showed the minimum attachment characteristics.

Typical electron beam and sustaining discharge current profiles are shown in Fig. 4. In the absence of any impurity detachment, the analysis of the experiment is extremely simple since the only electron loss mechanism is the electron-ion recombination process. Under these conditions, it can be readily shown that the electron density varies at $\tanh(\alpha n_{e_o} t)$ during the ionization portion of the profile and varies inversely as $1 + \alpha n_{e_o} t$ during the afterglow portion. Here n_{e_o} is the steady state electron density following the onset of the electron beam (see Fig. 4) and α is the electron-ion recombination rate coefficient. Diffusion effects can be neglected in the present experiment because of the

high neutral particle density and the large physical dimensions of the discharge region itself. These analytic electron density predictions are in good agreement with the experimental results in N_2.[14]

The presence of impurity attachment considerably complicates the analysis of the experiment. The following processes are assumed for purposes of experimental analysis:

$$e + AB^+ \rightarrow A + B + \Delta E \tag{1}$$

$$e + I \rightarrow I^- + \Delta E \tag{2}$$

$$I^- + AB^+ \rightarrow I + AB + \Delta E \tag{3}$$

In the above reactions, AB^+ is assumed to be the dominant positive ion and I the impurity species. The details of the attachment process which is probably via three-body stabilization are not important in the present analysis. Collisional detachment is not expected to be important because of the low ion energies which are approximately thermal. The electron and negative ion densities are now described by

$$\frac{dn_e}{dt} = S - \alpha n_e (n_e + n_-) - \beta n_e \tag{4}$$

$$\frac{dn_-}{dt} = \beta n_e - \gamma n_- (n_e + n_-) \tag{5}$$

where n_e and n_- are the electron and negative ion densities respectively, α is the two-body electron ion recombination rate coefficient, β is the overall attachment rate and γ is the ion-ion neutralization rate coefficient. The above equations also satisfy charge conservation. In these equations the source term S describes the rate of ionization by the primary electron beam and is directly proportional to the electron beam current.

Unfortunately, there are no analytical solutions to be above simultaneous equations. However, it is possible to obtain approximate solutions provided the attachment term is small compared with the electron-ion recombination rate, i.e. $\beta \ll \alpha n_{e_o}$. This was true for the experimental conditions considered here. Under these conditions the density of negative ions is small compared to the electron density except at long times in the afterglow. The electron rate equation (4) can then be intergrated in the afterglow region to give

$$\frac{n_{e_o}}{n_e} = \left(\frac{\alpha n_{e_o} + 1}{\beta'}\right) e^{\beta' t} - \frac{\alpha n_{e_o}}{\beta'} \qquad (6)$$

where $\beta' = \beta + \alpha n_{-_o}$ and n_- is assumed to be approximately constant as verified by numerical integration of Eqs. (4) and (5). The subscript o refers to the steady state conditions prior to the afterglow. The result is valid except for long times until $\alpha n_e \sim \beta$ and attachment then dominates the afterglow. For vanishingly small attachment coefficient, Eq. (6) leads to the expected result

$$\frac{n_{e_o}}{n_e} = 1 + \alpha n_{e_o} t$$

By expansion of Eq. (6) it can be seen that the current decay in the afterglow will have an initial linear slope $\alpha n_{e_o} + \beta'$ and will subsequently decay at an increasingly faster rate due to the impurity attachment. This is evident in the experimental results shown in Fig. 5. Both β' and $\alpha n_{e_o} + \beta'$ can be derived from a quadratic fit to the experimental data in the initial afterglow region.

With the approximation $\beta \ll \alpha n_{e_o}$ and $n_- \ll n_e$ it is also possible to integrate Eq. (4) during the initial ionization process and so derive

$$\frac{n_e}{n_{e_o}} = \tanh (\alpha n_{e_o} + \beta) t \qquad (7)$$

where the source term S is approximated by the steady state conditions $S = \alpha n_{e_o}^2 + \beta n_{e_o}$. It is therefore possible to derive αn_{e_o} from the discharge current variation during the onset of ionization provided that β is known. Thus, it is possible to check the value of αn_{e_o} obtained in both the onset and afterglow regions. In principle, one could determine the attachment coefficient β by measuring the slope of the exponential decay in the discharge current long times. However, this requires a very accurate measurement of the electron current and this was beyond the scope of the experiment.

In order to determine the steady state electron density, n_{e_o}, from the discharge current density measurements, it is necessary to know the electron drift velocity. This can be obtained from previous swarm measurements or by solving the Boltzmann equation for the electron interaction with the gas using cross section data previously measured by [15]

Schultz[16] and inferred by Hake and Phelps.[17] The latter approach fits the experimental swarm data and can be used to predict the average electron energy.

As a check on the simplified analysis described above, the exact equations were solved numerically using the values of α and β deduced from the above analysis and an assumed value of γ in the range from 2×10^{-7} to 2×10^{-6} cm^3/sec. Excellent agreement with the approximations (6) and (7) was obtained over the entire current profile for ion-ion neutralization rates, γ, of the order of 10^{-6} cm^3/sec. This value is not unreasonable in view of the experimental measurements in ion-ion neutralization in oxygen[18] and air[19] at densities of the order of one amagat.

RESULTS AND DISCUSSION

The summary of the experimentally derived values for α is shown in Fig. 6 as a function of the average electron energy. The experimental results are shown for the four different pressures used in the experiment and in addition a vertical line is shown through each experimental point to indicate the difference in α as deduced from the afterglow and from the onset characteristics. In all cases, the analysis of the afterglow data lead to a higher value of α than the analysis of the onset data with this difference decreasing with pressure as is evident from Fig. 6. The measured recombination rate coefficients lie in the range 10^{-7} to 10^{-6} cm^3/sec and are typical of dissociative recombination rates measured in other diatomic molecules.[2-4] Based on the measurements of Chong and Franklin[7] and McDaniel, et. al.[8] it is assumed that the dominant ion was either the dimer ion $C_2O_2^+$ or a higher order polymer ion as a result of the very large rate for the three body conversion of CO^+ to $C_2O_2^+$ as well as the experimentally observed large equilibrium constant. Some evidence for higher order polymers of the CO ion is given by the apparent increase of the recombination rate with increasing pressure. This might be interpreted as indicating a change in the equilibrium ion concentration amongst the possible polymer ions as a function of pressure since the individual polymer ions are not expected to exhibit the same rate of dissociative recombination.

The discrepancy between the recombination rate results obtained from the afterglow and the onset characteristics at high pressures is somewhat puzzling. It should be pointed out however that the accuracy

of the determination of α decreases with increasing pressure. This is primarily due to the increase in the effective attachment rate at high pressures. The difference in the derived values of α between the onset and afterglow could also be accounted for by a small but finite rise time in the switch-on characteristics of the electron beam. A rise time of the order of 1 microsecond is more than sufficient to account for this difference in the 700 Torr experiments. Such a small rise time would not have been resolved with the existing instrumentation on the electron gun. A finite rise time of this order of magnitude would not affect the low pressure results because of the slower electron decay at low pressures. This results from the smaller attachment rate and the decrease in n_{e_o} with pressure for a fixed energy electron beam.

The recombination rate data shows a fairly steep temperature dependence approximately $T_e^{-1.6}$ where T_e is equivalent temperature associated with the average electron energy. Such large temperature variations have been observed in previous shock tube experiments in the noble gas dimer ions[20] and in shock tunnel experiments in N_2 [21] and CO.[22] These experiments were performed at high temperatures with the same electron and ion vibrational temperatures. These high temperature data have been explained as resulting from the dependence of the recombination cross section on the vibrational state of the ions.[1] It has been suggested by several authors that the recombination cross section decreases[23] rapidly with increasing vibrational quanta number of the initial ion. This argument may not be valid in the present experiments. Since the degree of vibrational excitation of the background CO increases linearly with time, due to the direct excitation of the

vibrational mode by electron impact, it might be expected that the vibrational excitation of the ions would increase with time due to collisional transfer of vibrational energy. However, the experimentally derived recombination rates from both the onset and the afterglow regions show the same temperature dependence within the experimental error. An alternate explanation for this temperature dependence was suggested by Bardsley[24] who discussed the possibility of indirect recombination rather than direct dissociative recombination. This indirect recombination is thought to proceed first to an excited Rydberg state which is followed by a two-step predissociation of this state. This process may be important in the dimer and polymer molecular ions although there does not appear to be any substantial experimental verification of this process.

The only other experimental data in CO which may be directly compared with the present are the results of Mentzoni and Donohoe[5, 6] taken at low temperatures and the shock tube measurements of Dunn.[22] All these experiments were performed under conditions where the dominant positive ion was thought to be CO^+ and as a result directly comparison with the present data is not valid. It is interesting to observe however that the high temperature shock tube data of Dunn which are plotted on Fig. 6 as the hatched region show a similar temperature dependence in the present data whilst lying a factor of 2 lower than the overall rate coefficient.

REFERENCES

1. J. N. Bardsley and M. A. Biondi, Advances in Atom. and Molecular Physics, Ed. D. R. Bates and I. Esterman, Academic Press, New York (1970).

2. W. H. Kasner and M. A. Biondi, Phys. Rev. 137, A317 (1965).

3. W. H. Kasner and M. A. Biondi, Phys. Rev. 174, 139 (1968).

4. C. S. Weller and M. A. Biondi, Phys. Rev. 172, 198 (1968).

5. M. H. Mentzoni and J. Donohoe, Phys. Lett. 26A, 330 (1968).

6. M. H. Mentzoni and J. Donohoe, Can. J. Phys. 47, 1789 (1969).

7. S. L. Chong and J. L. Franklin, J. Chem. Phys. 54, 1487 (1971).

8. E. W. McDaniel, J. H. Shummers, G. M. Thomson, I. R. Gatland, D. R. James and F. Graham, Third International Conference on Atomic Physics, August 7, 1972, p. 167.

9. M. M. Mann, W. B. Lacina and M. L. Bhaumik, 7th International Quanta Electronics Conference, Montreal, Canada (1972).

10. R. E. Center and G. E. Caledonia, 25th Annual Gaseous Electronics Conference, London, Ontario (1972).

11. A. Mandl, S. A. Fogelson and S. D. Hester, AIAA 5th Fluid and Plasma Dynamics Conference, Paper 72-676 (1972).

12. A. Cohen and G. E. Caledonia, J. App. Phys. 41, 3767 (1970).

13. T. G. Lee, J. Phys. Chem. 67, 360 (1963).

14. D. H. Douglas-Hamilton, Avco Everett Research Laboratory Research Report 343,(1972).

15. W. L. Nighan, App. Phys. Lett. 20, 96 (1972).

16. G. J. Schulz, Phys. Rev. 135, A 988 (1964).

17. R. D. Hake, Jr. and A. V. Phelps, Phys. Rev. 158, 70 (1967).

18. S. McGowan, Can. J. Phys. 45, 439 (1967).

19. W. Mächler, Z. Physik, 104 1 (1936).

20. A. J. Cunningham and R. M. Hobson, Phys. Rev. 185, 9[illegible] (1969).

21. M. G. Dunn and J. A. Lordi, AIAA 8, 339 (1970).

22. M. G. Dunn, AIAA 9, 2184 (1971).

23. T. G. O'Malley, Phys. Rev. 185, 101 (1969).

24. J. N. Bardsley, J. Phys. B. 1, 365 (1968).

FIGURE CAPTIONS

Fig. 1 Schematic outline of the one meter high pressure CO laser.

Fig. 2 Photograph of lasing cavity and electron gun housing.

Fig. 3 Schematic of experimental apparatus for the electron-ion recombination measurements.

Fig. 4 Typical electron beam and discharge current profiles. Data taken at p_{CO} = 350 Torr and $E/N = 1.0 \times 10^{-16}$ volt-cm^2.

Fig. 5 Experimental data in the afterglow region for a CO pressure of 200 Torr.

Fig. 6 Summary of electron-ion recombination rate data in pure CO.

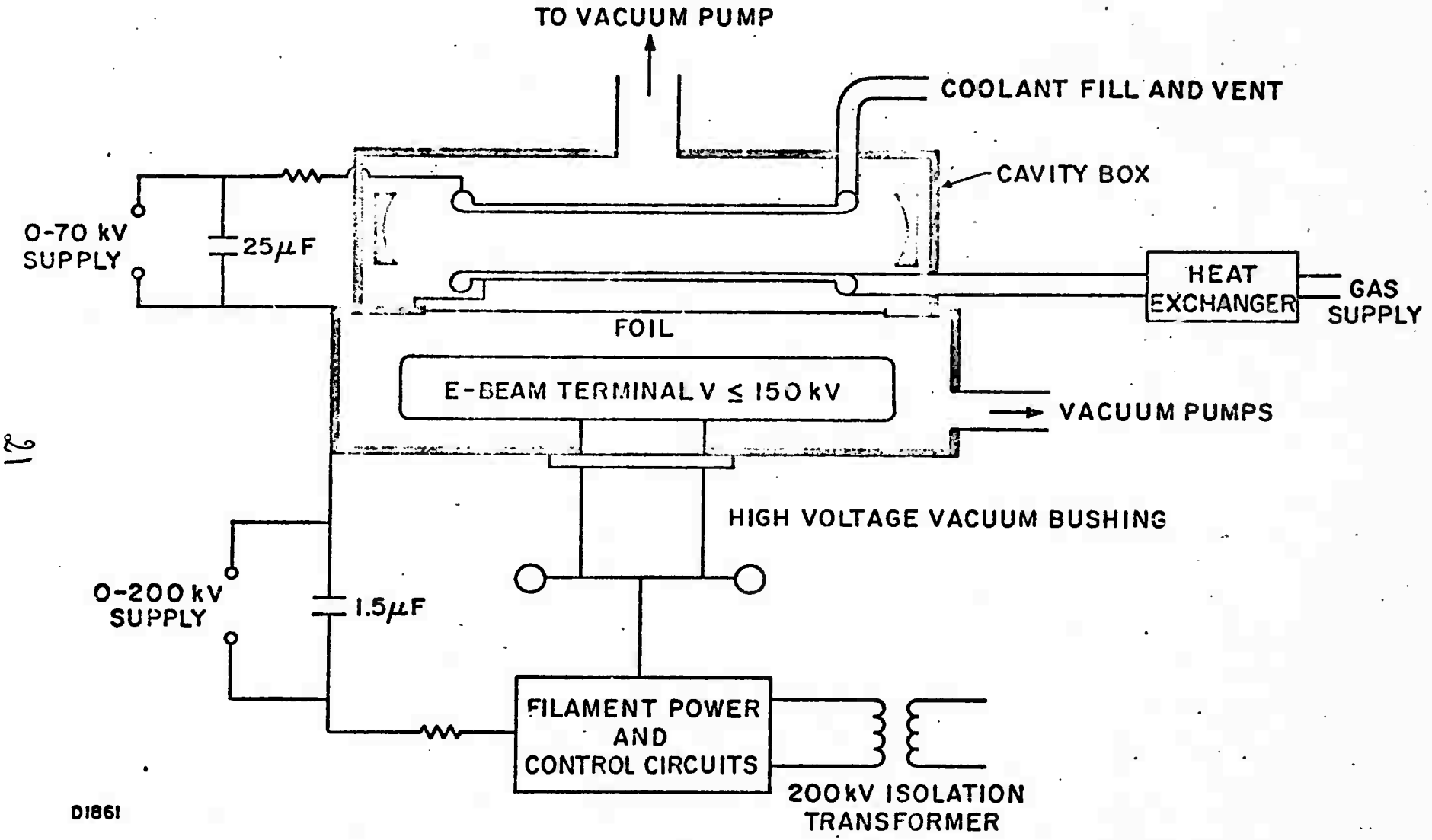

FIG. 1 SCHEMATIC OF 1 ATM. CO LASER

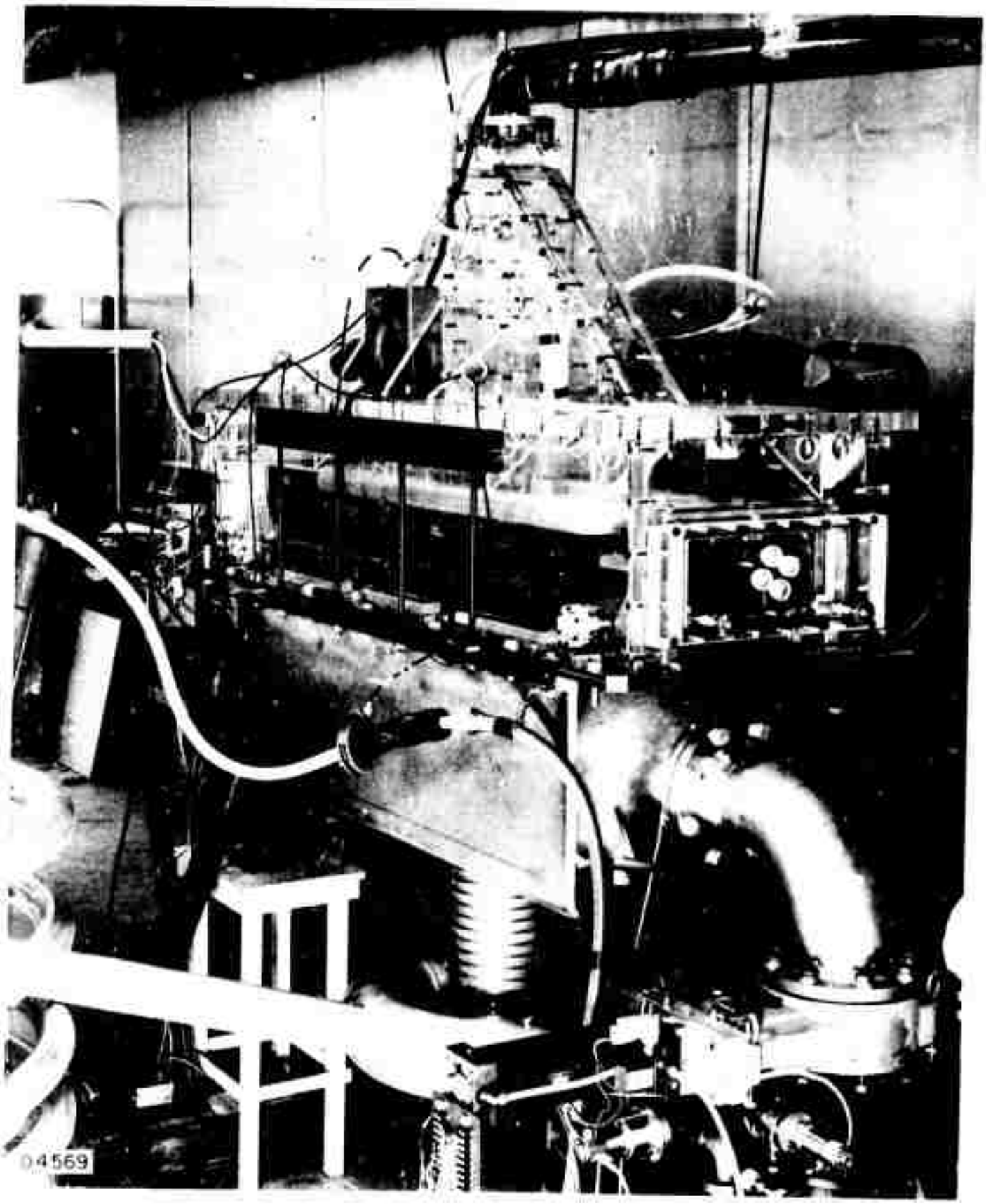

Fig. 2

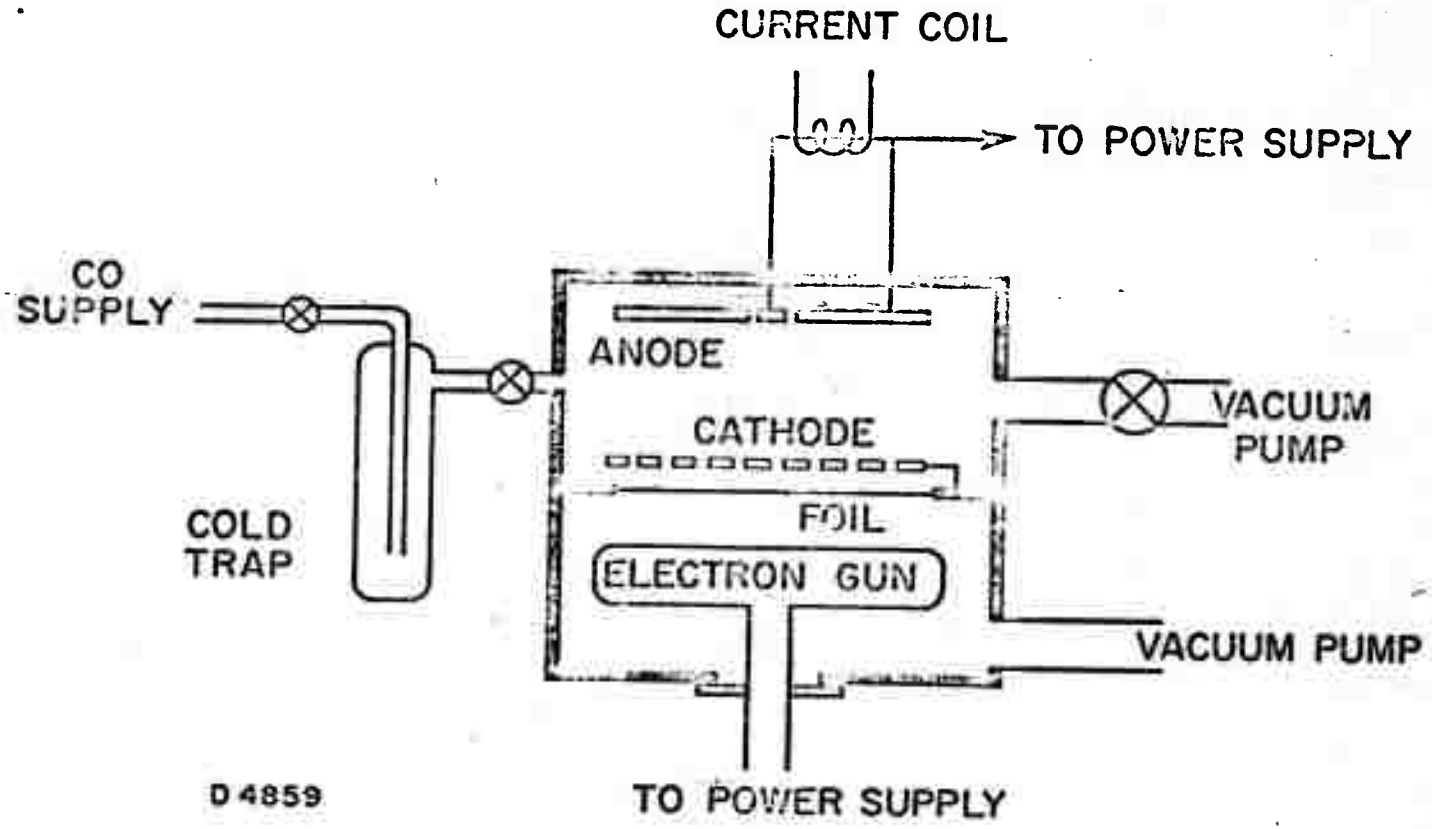
CURRENT COIL
TO POWER SUPPLY
CO
SUPPLY
ANODE
CATHODE
VACUUM
PUMP
FOIL
COLD
TRAP
ELECTRON GUN
VACUUM PUMP
D 4859
TO POWER SUPPLY

Fig. 3

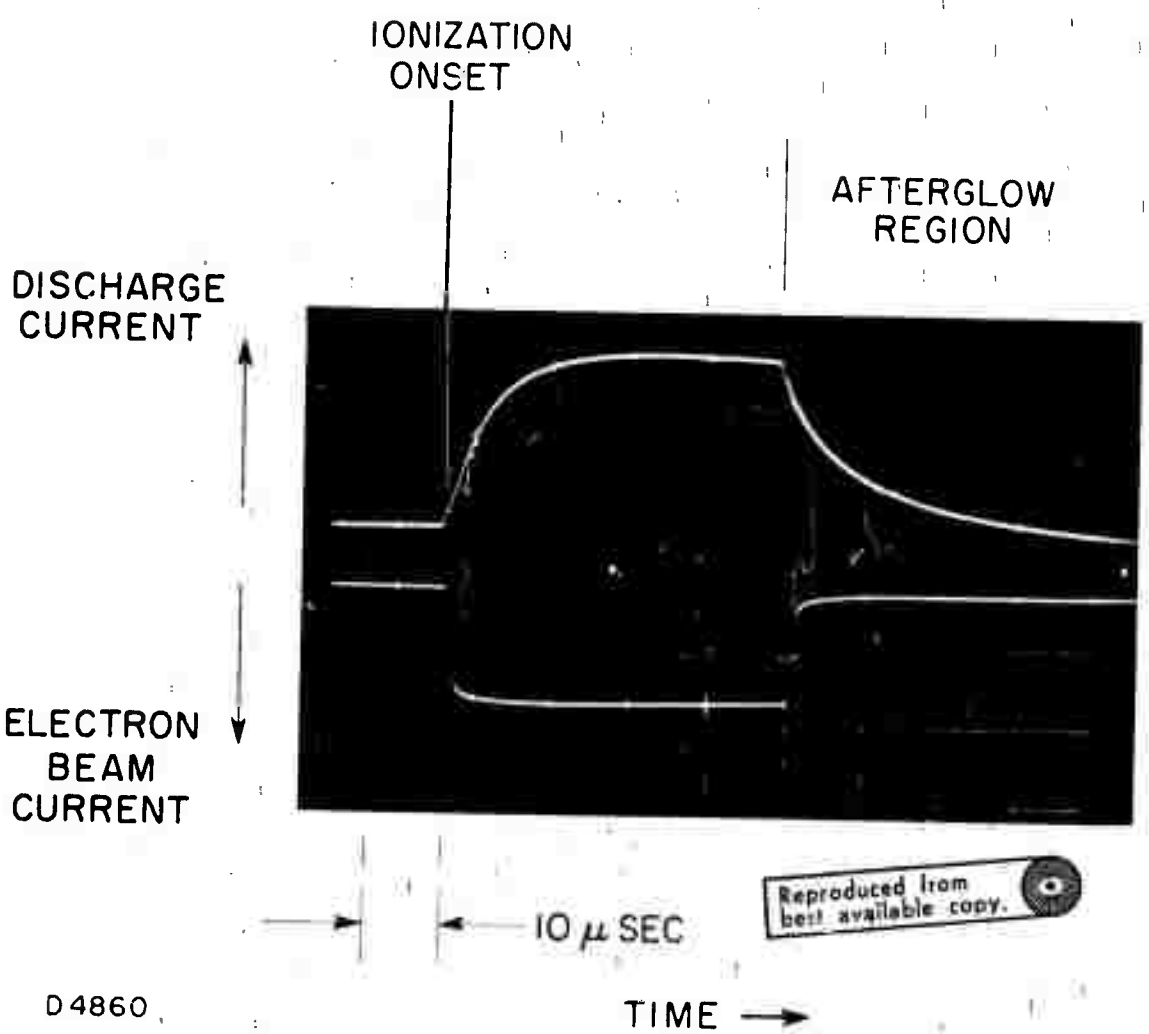

Fig. 4

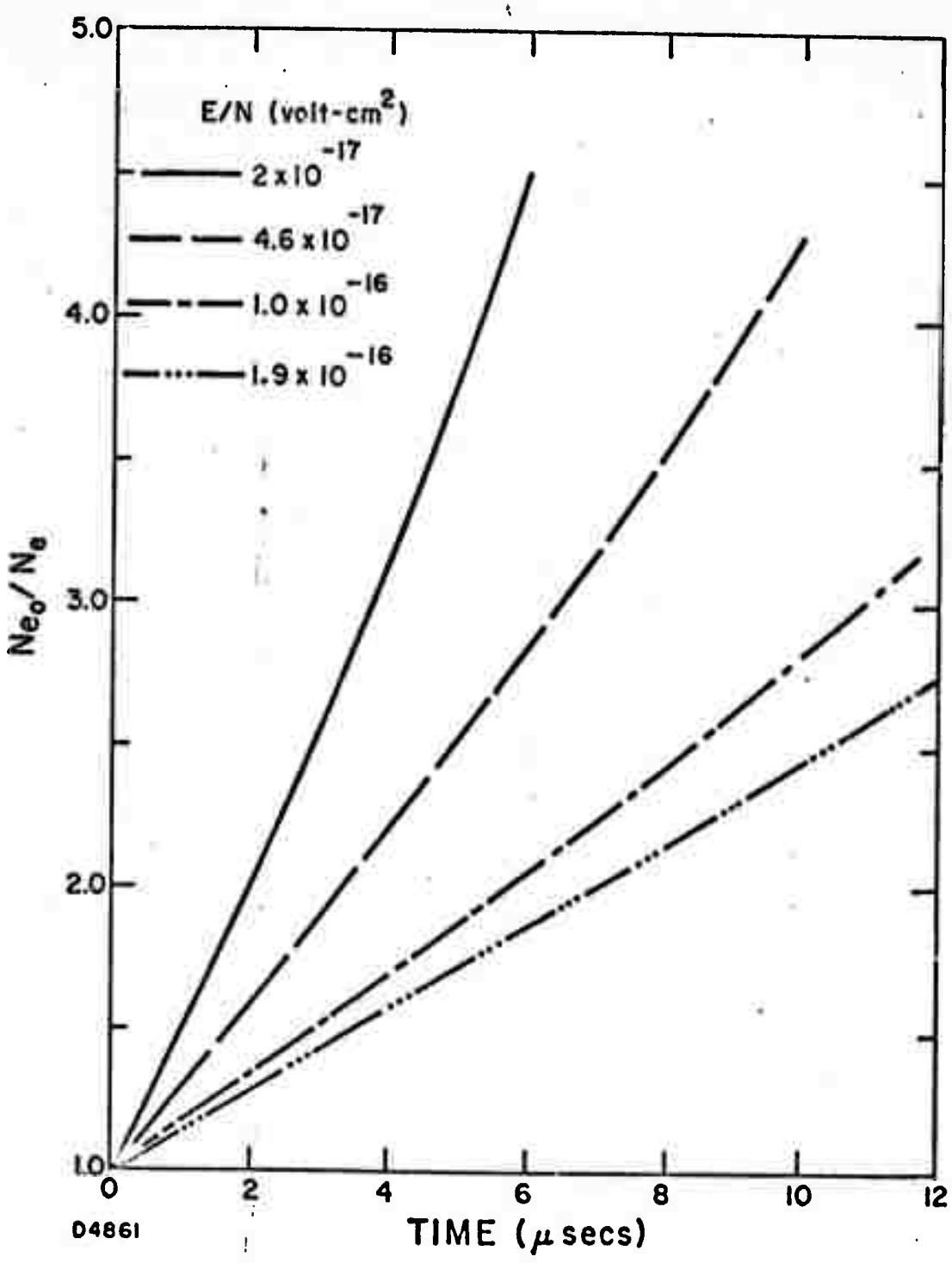
E/N (volt-cm^2)
2×10^{-17}
4.6×10^{-17}
1.0×10^{-16}
1.9×10^{-16}
N_{e_o}/N_e
5.0
4.0
3.0
2.0
1.0
0
2
4
6
8
10
12
TIME (μ secs)
04861

Fig. 5

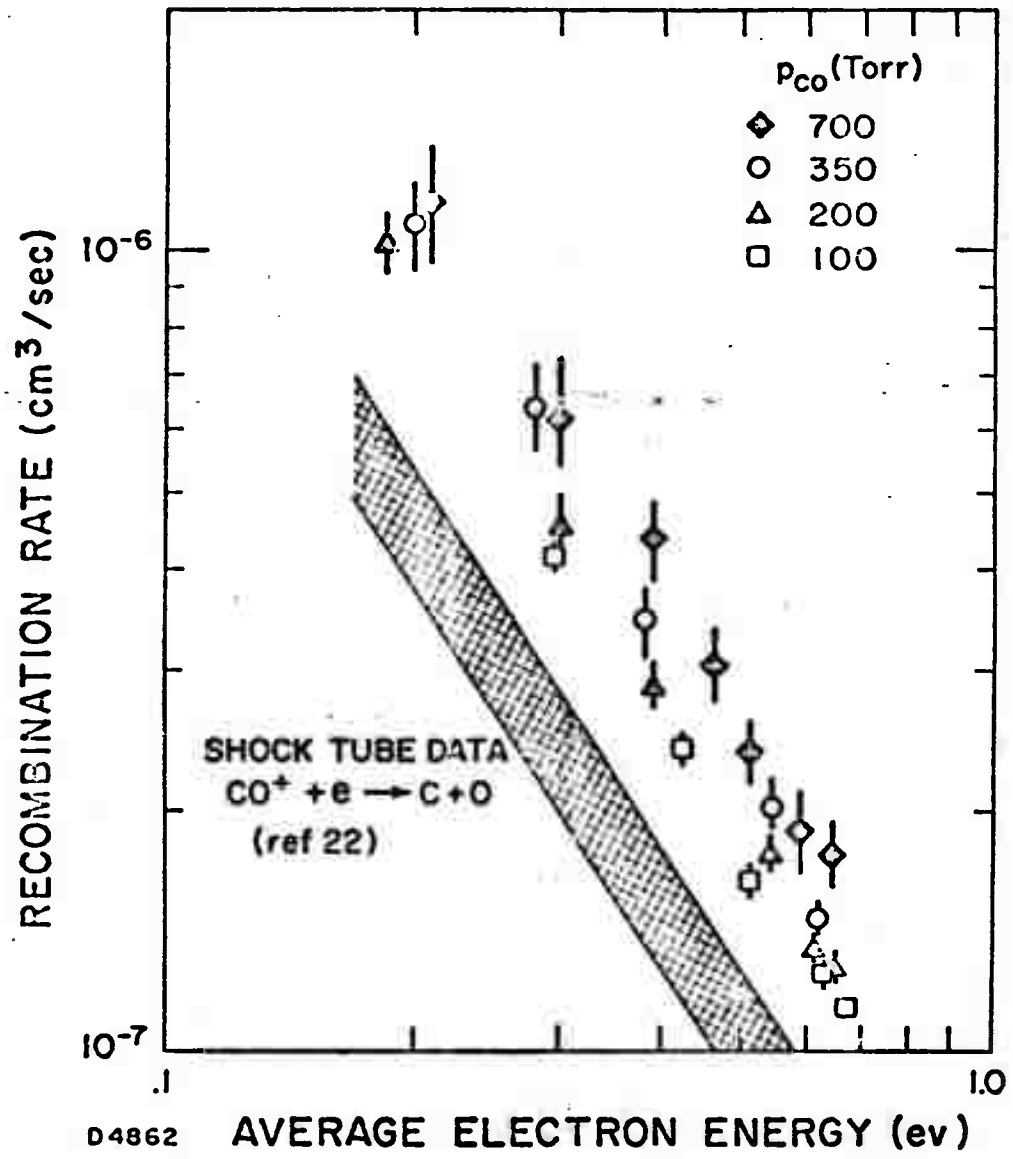
p_{CO}(Torr)
700
350
200
100
10^{-6}
10^{-7}
RECOMBINATION RATE (cm^3/sec)
SHOCK TUBE DATA
$CO^+ + e \rightarrow C + O$
(ref 22)
.1
1.0
D4862
AVERAGE ELECTRON ENERGY (ev)

Fig. 6